High-capacity Directly-Modulated Optical Transmitter for 2-µm Spectral Region

Zhixin Liu, *Member, IEEE*, Yong Chen, Zhihong Li, Brian Kelly, Richard Phelan, John O'Carroll, Tom Bradley, John P. Wooler, Natalie V. Wheeler, Alexander M. Heidt, Thomas Richter, Colja Schubert, Martin Becker, Francesco Poletti, *Member, IEEE*, Marco N. Petrovich, Senior *Member, IEEE*, Shaif-ul Alam, David J. Richardson, *Fellow, IEEE*, and Radan Slavík, Senior *Member, IEEE*

***Abstract*—The 2-µm wave band is emerging as a potential new window for optical telecommunications with several distinct advantages over the traditional 1.55µm region. First of all, the Hollow-Core Photonic Band Gap Fiber (HC-PBGF) is an emerging transmission fiber candidate with ultra-low nonlinearity and lowest latency (0.3% slower than light propagating in vacuum) that has its minimum loss within the 2-µm wavelength band. Secondly, the Thulium-doped fiber amplifier that operates in this spectral region provides significantly more bandwidth than the Erbium-doped fiber amplifier. In this paper we demonstrate a single-channel 2-µm transmitter capable of delivering >52 Gbit/s data signals, which is twice the capacity previously-demonstrated. To achieve this we employ discrete multi-tone (DMT) modulation via direct current modulation of a Fabry-Perot semiconductor laser. The 4.4-GHz modulation bandwidth of the laser is enhanced by optical injection locking, providing up to 11 GHz modulation bandwidth. Transmission over 500-m and 3.8-km samples of HC-PBGF is demonstrated.**

***Index Terms*— Optical fiber communication, Optical transmitter, Optical modulation, Digital signal processing, Photonic band gap fiber.**

I. Introduction

THE capacity of optical communication networks has grown exponentially over the past few decades, leading to today's global communication systems and the ubiquitous internet. This growth has been enabled by many technological breakthroughs including low-loss, single mode transmission fiber (SMF), the erbium-doped fiber amplifier (EDFA), wavelength division multiplexing (WDM), and more recently digital signal processing (DSP) combined with coherent detection. Throughout this technological evolution, silica-based single mode optical fiber has been used as the transmission medium. For long distance and large-capacity transmission, most work has been done within the 4-5 THz bandwidth of the C-band telecommunication window where the fiber transmission loss is at a minimum and low-noise amplification is available. The advanced modulation format signaling allows significant increase of capacity within this limited bandwidth. However, the capacity-transmission distance product is ultimately limited by fiber nonlinearity [1]. The record reported transmission capacity for SMF is now within about a factor of 2 of its theoretical maximum defined by the nonlinear Shannon limit [2]-[3]. However, as a result of the exponentially increasing volume of internet traffic, today's telecom networks are rapidly being driven towards their capacity limits, sparkling concerns over a potential future "capacity crunch" [4]. To keep pace with the increasing traffic demand at a reasonable cost-per-bit, new physical layer technology for communication networks will soon be necessary. In the search for solutions, the research community is investigating various new approaches [5]. For instance, mode division multiplexing assisted by MIMO (Multiple-Input-Multiple-Output) signal processing has recently attracted much interest and shown impressive data transmission performance [6].

Further opportunities are provided by a radically new form of transmission fiber, the Hollow-Core Photonic Band Gap Fiber (HC-PBGF), which guides light in a hollow core by virtue of photonic bandgap effects determined by a carefully designed glass microstructure [7]. The HC-PBGF has a number of intriguing optical properties relevant to optical communications, including ultralow optical nonlinearity, excellent power handling capabilities, low latency, and even offers the prospect of ultralow losses within around 2.0 µm spectral region, where its loss is predicted to be similar to - if not lower than - that of conventional SMF at 1.55 µm [8]. Such a combination of advantages relative to conventional solid core silica optical fibers points to an exciting vision of future optical communications. In addition to HC-PBGF, it is also worth noting that other glass systems exist with potential for losses as low as 0.1 dB/km at wavelengths around 2 µm [9], providing

Z. Liu, Y. Chen, Z. Li, T. Bradley, J. P. Wooler, N. V. Wheeler, A. M. Heidt, F. Poletti, M. N. Petrovich, S. Alam, D. J. Richardson, and R. Slavík are with the Optoelectronics Research Centre, University of Southampton, Southampton, United Kingdom, SO17 1BJ. (e-mail: z.liu@soton.ac.uk).

B. Kelly, R. Phelan, and J. O'Carroll are with Eblana Photonics, Dublin, Ireland.

T. Richter and C. Schubert are with the Fraunhofer Institute for Telecommunications, Heinrich Hertz Institute, Einsteinufer 37, 10587 Berlin, Germany.

M. Becker is with the Leibniz Institute of Photonic Technology, Jena, Germany.

This research has received funding from EPSRC Fellowship grant agreement no. EP/K003038/1. The HC-PBGF, Tm-doped amplifier, and semiconductor lasers used in these experiments were developed within EU FP7 project MODE-GAP (grant agreement 258033) or EPSRC grant EP/I061196X (HYPERHIGHWAY).

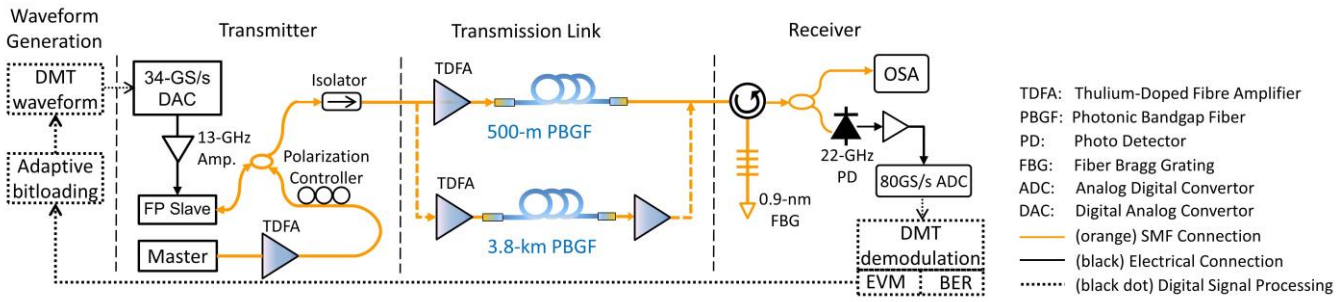

Fig. 1. Transmission experiment setup.

yet further motivation to consider the telecommunications potential at 2 µm.

Another key requirement for optical transmission systems is the availability of a high gain, low noise optical amplifier, which largely determines the total system bandwidth. Fortunately, the Thulium (Tm^{3+}) doped fiber amplifier (TDFA) offers a route to significantly enhanced amplification bandwidths around 2µm. The remarkably broad emission spectrum of the $^3F_4 - {}^3H_6$ transition in Tm-doped silica covers about 30 THz (~1700 to ~2100 nm [10]) and was shown to give about 22 THz (1830-2050 nm) amplification bandwidth in a single device [11]-[12], more than two times that of the Erbium doped fiber amplifier (EDFA) of similar configuration/complexity. Through more complex TDFA designs amplification has been demonstrated over the full 30 THz bandwidth, with further extension still possible.

Key components such as narrow linewidth lasers [13], external modulators, optical hybrids [14], high-speed photo detectors [15], as well as many passive components have already been developed for 2 µm region. With the availability of these building blocks, 2 µm fiber transmission systems have now been demonstrated and the transmission capacity has been consistently improved, although all experiments to date have been limited to simple data coding only. First, OOK signal generation using an external modulator at a data rate of up to 8.5 Gb/s combined with 3-channel Fast-OFDM binary phase shift keying (BPSK) signals via direct laser modulation (5 Gb/s) were demonstrated, resulting in a total capacity of 20 Gbit/s transmitted over 50 m of standard single mode fiber [16]. Following that 4-channel transmission of 16 Gb/s signals over 290 m of HC-PBGF was demonstrated [17]. Recently, 8-channel coarse WDM transmission over 1.15 km of HC-PBGF was shown using 4-channel 12.5 Gb/s OOK external modulation and 4-channel 7.7 Gb/s 4-ASK Fast-OFDM direct modulation [18], providing a total capacity of 81 Gb/s. As can be seen, the single channel capacity in these previous demonstrations was relatively low, since the existing components have limited bandwidth (e.g., modulators, directly-modulated lasers). To scale up the single channel capacity, we recently demonstrated a directly modulated optical injection locking (OIL) based transmitter capable of generating 64-level quadrature amplitude modulation (64-QAM, 30 Gb/s) signals using discrete multi-tone (DMT) modulation. After transmission over 500m HC-PBGF, a sub-FEC data rate of 25 Gbit/s (using 32QAM-DMT) was obtained [19].

In this paper, we demonstrate more than double this capacity, obtained by improving our transmitter on several fronts. First, we used DMT with adaptive bit loading, which was recently shown to enable >100 Gb/s transmission at both 1310 nm and 1550 nm [20] spectral regions. This new approach is implemented using DSP and leads to maximized capacity for a given bandwidth and signal quality. Further, it makes the transmitter low-cost, as it is based on simple direct modulation + direct detection only. Further improvements in our technique [19] include optimization of the optically-injected power and frequency detuning for injection locking, which we present here. Subsequently, we demonstrated transmission over two HC-PBGF samples of 500-m and 3.8-km length respectively, showing that the bit-loading DMT is particularly suitable for high-speed transmission using current state-of-the-art HC-PBGFs. To the best of our knowledge the 3.8-km HC-PBGF sample which we designed and fabricated in house represents the longest single continuous length of HC-PBGF tested to date in a transmission experiment. Such a fiber length is already more than adequate for many potential short haul communication needs (for instance for low latency transmission within a data center).

II. Transmission Experiment Setup

Fig. 1 shows our experimental setup. The waveform samples of the DMT signal are generated offline based on a PRBS of 2^{18}-1 length and an inverse Fourier Transform size of 1024. The modulation format for each sub-carrier is assigned by the bit loading algorithm. A 16-sample cyclic prefix (CP) is placed both before and after each symbol. A clipping ratio of 3.2 (3.2 times standard deviation of the original waveform) was used for optimal performance.

We used two Arbitrary Waveform Generators (AWGs) of different specifications for generating our signal – their characteristics are summarized in Table 1. Here we see a trade-off between the two AWGs in terms of their bandwidth and effective number of bits (ENOB). Whilst allowing a comparison of performance, the main reason for using two AWGs in our experiments was that the longer HC-PBGF

TABLE I
Parameters of the Used AWGs

	Low-bandwidth AWG	High-bandwidth AWG
RF Bandwidth	9.6 GHz	17 GHz
Resolution	8 bits	6 bits
ENOB	6.5 bits	4.5 bits
Sampling rate	24 GS/s (interleaved)	34 GS/s

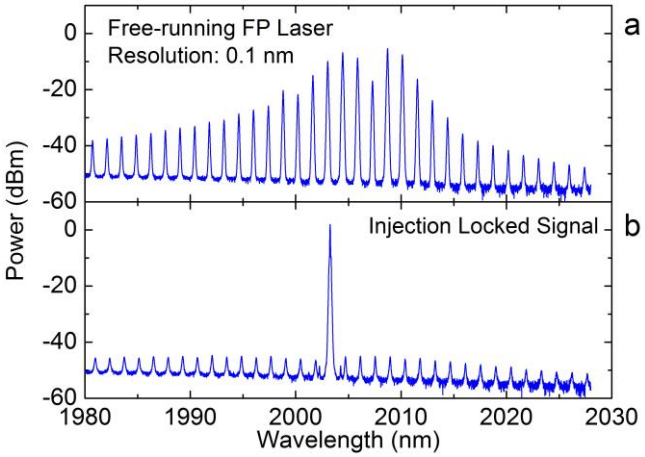

Fig. 2. Optical spectrums of the FP laser with (b) and without (a) OIL.

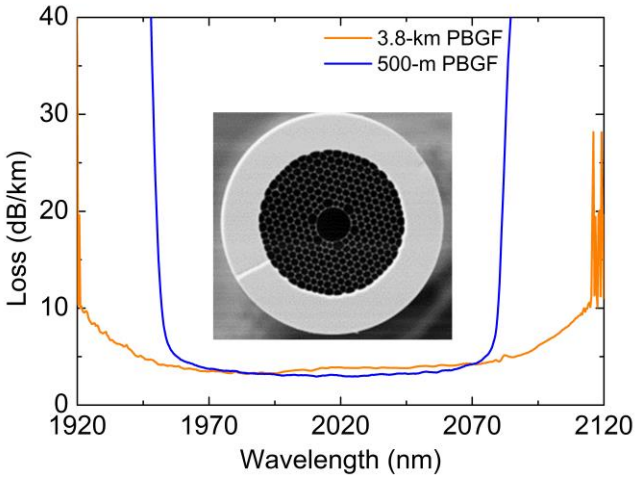

Fig. 3. Insertion loss of the HC-PBGF samples. Blue: 500-m PBGF sample. Orange: 3.8-km PBGF sample.

sample was not available at the same time as the (loaned) larger-bandwidth AWG.

Using the high-bandwidth AWG, the subcarrier bandwidth was 13.7 MHz and the waveforms were digitally up-converted to a 7-GHz RF carrier frequency, which resulted in an electrical bandwidth of 14 GHz. When the low-bandwidth AWG was used, the subcarrier bandwidth was 9.4 MHz and signal was up-converted to a 4.8-GHz RF carrier, providing a total bandwidth of 9.6 GHz. Due to the limited ENOB, no pre-emphasis was implemented to compensate for the electrical roll-off of the AWGs.

The directly modulated laser used as the slave laser was an $In_{0.75}Ga_{0.25}As$ Fabry-Perot laser diode (FP-LD) in a butterfly package with its output directly coupled into a polarization-maintaining (PM) fiber without any in-built isolator (as necessary for the OIL). The master laser was an $In_{0.75}Ga_{0.25}As$ multiple quantum-well discrete-mode laser diode [13] with in-built dual-stage isolator emitting 3 dBm of CW light at 2003.4 nm. In our experiments we found that the highest back-to-back capacity required slightly larger master laser power (7-8 dBm). Thus, we amplified the master laser using a single-stage TDFA. A polarization controller (PC) followed by a 60:40 split ratio PM fiber coupler used for the OIL. As shown in Fig. 2, the free-running directly-modulated slave laser emits more than 30 longitudinal modes. After the OIL, the side modes were suppressed by more than 45 dB.

To maintain good modulation linearity after OIL, the slave laser was biased slightly above its free-running threshold at 25 mA and was modulated by electrical DMT signals with a peak-to-peak voltage of 1.8 Volts (average power of 2 dBm).

Before launching the signal into the transmission fiber, the transmitter power was boosted to 15 dBm using a home-built dual-pump TDFA [11]. Two samples of HC-PBGFs were used in the experiment. The measured insertion loss over 1920-2120 nm is shown in Fig. 3. The first is a 500m long sample of 19-cell core HC-PBGF with a loss of ~2.5 dB/km at 2001nm, and a 3-dB transmission bandwidth of 122 nm (1954-2076nm). The second is again a 19-cell core HC-PBGF but length in this case is a record 3.8 km. The fiber has in this case a minimum loss of ~ 3 dB/km at 2010 nm and a remarkable width bandwidth of 160 nm (1936-2096nm). Further details of this fiber are given in [21]. Both samples were pigtailed with SMF-28 with an estimated splice loss of 3 dB at each end arising primarily from mode-mismatch. Note that this value could be reduced through use of more optimized splicing procedure. As the pigtailed 3.8 km HC-PBGF had a total insertion loss of 17 dB, another TDFA with 10 dB gain was used at its output in the optically-preamplified receiver.

At the receiver side a band-pass filter (fiber Bragg grating (FBG) with a 3 dB bandwidth of 0.9-nm) was used to remove the out-of-band ASE noise. The filtered light was then split for spectrum/power monitoring and direct detection. A 22 GHz, 2-μm reverse-voltage-biased photodiode (Discovery Semiconductor DSC2-30S) in conjunction with an RF amplifier (13 GHz bandwidth) was used for direct detection. The signal was then sampled at 80 GS/s by an Agilent DSO-X 93204A real-time oscilloscope. Demodulation was implemented using offline DSP.

To calculate the bit loading, we used a DMT signal with Quadrature Phase Shift Keying (QPSK) and identical power on all sub-carriers as a probe. The bit loading for each subcarrier was estimated by measuring the error-vector magnitude (EVM) of the received probe signal followed with dynamic bit adaption. The bit-loading algorithm we used is a modification of Chow's algorithm [22] such that the total capacity is maximized at a bit-error ratio (BER) target of 3.8×10^{-3} for 7% forward error correction (FEC) threshold [23]. The BER was determined based on error counting of the demodulated bit loaded DMT signal.

III. Results and Discussion

A. *Transmitter Frequency Response*

The modulation characteristics/bandwidth of a laser under OIL depends on the frequency difference Δf between the carrier frequency of the master laser (f_{master}) and the carrier frequency of the free running slave laser mode (f_{slave}) [24], [25]. It also depends on the power injected from the master. In our experiment, f_{master} was constant while f_{slave} was controlled via the temperature of the slave laser. We set the injected power to 4 dBm, as above this power we started to

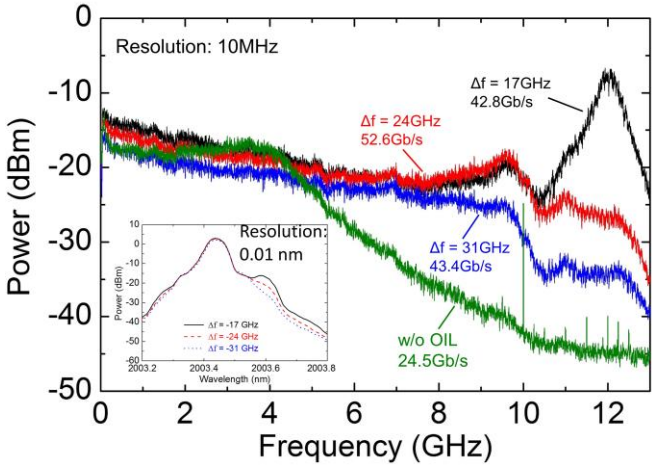

Fig. 4. RF spectra of the DMT signal. Olive: without OIL; Blue: Δf = 31GHz; Red: Δf = 24GHz; Black: Δf = 17GHz at different frequency detuning. (Inset: Optical spectra of the DMT signal at different frequency detuning.)

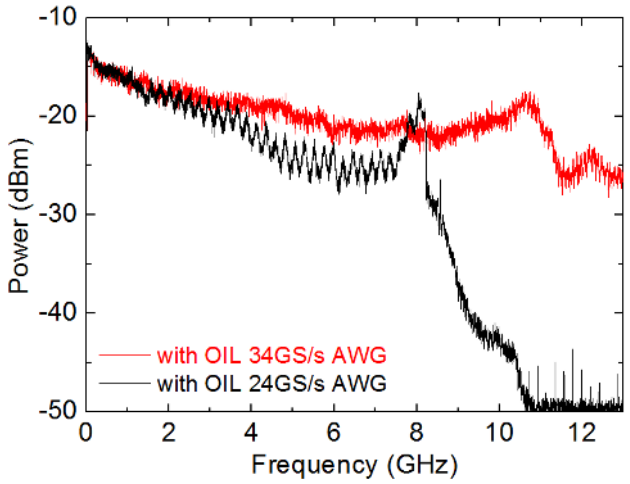

Fig. 5. Electrical spectra of back-to-back signals. Red: using the high-bandwidth AWG; Black: using the low-bandwidth AWG.

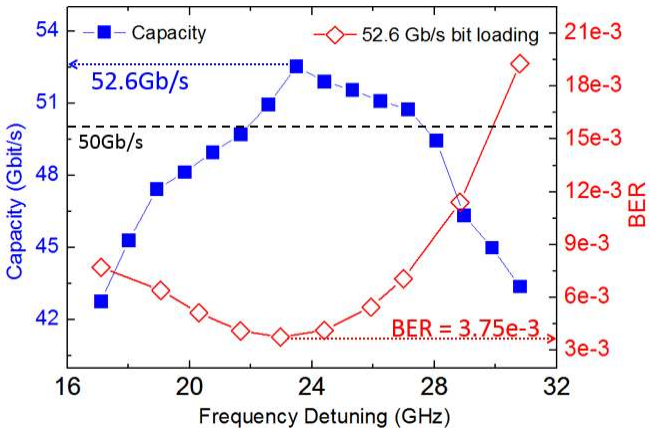

Fig. 6. Impact of frequency detuning on the signal performance: closed square: capacity, open diamond: BER for 52.6 Gb/s bit loading.

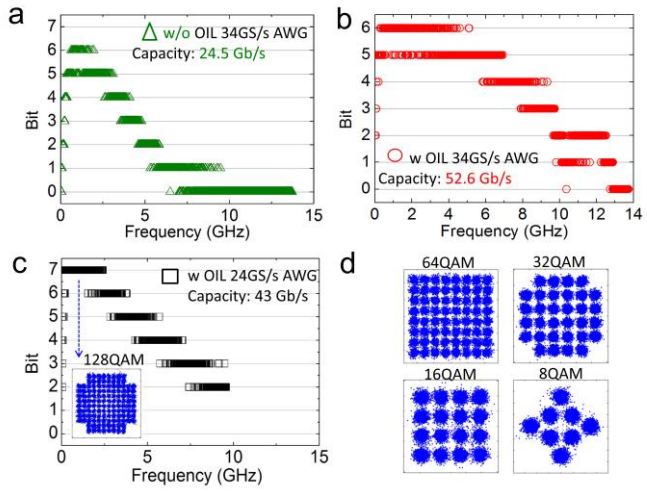

Fig. 7. Bit loading for back-to-back DMT signal using the high-bandwidth AWG (each point represents one sub-carrier and shows how many bits-per-symbol it carries) (a) without OIL and (b) with OIL. (c) Bit loading using the low-bandwidth AWG with OIL. (d) Constellation diagrams of the demodulated signal for different subcarrier modulation.

observe some instability in the OIL process. For lower powers, we achieved smaller transmission capacity, which was a consequence of a smaller locking range [24]. The optical spectra generated using the higher-bandwidth AWG and corresponding electrical spectra after direct detection when Δf was varied from 17 to 31 GHz (the region that gave the best performance in terms of the transmission capacity discussed later) are shown in Fig. 4.

The green curve in Fig.4 shows the spectra of the received back-to-back (BtB) DMT signal without any OIL: the 3 dB modulation bandwidth was only 4.4 GHz with a fast roll-off at higher frequencies. With the OIL, we observed a remarkable enhancement of the modulation bandwidth due to the photon-to-photon interaction due to OIL [24]. At a Δf of 31 GHz, the signal spectrum has a smooth roll-off, which is similar to the roll-off of the AWG's electrical output. At $\Delta f$of 17 GHz, we observed a strong relaxation oscillation at 12 GHz. According to theory [25] small Δf results in a sharp relaxation oscillation resonance, which leads to a strong modulation response at high frequencies. A larger detuning frequency leads to a damped relaxation oscillation resonance that manifests itself as a broad relaxation oscillation peak of limited strength. Indeed, there is an optimum between these two that provide a maximally flat and large modulation bandwidth, which – as we show later (Fig. 6) leads to the maximum data capacity that can be achieved. As shown in Fig. 4, we achieved (for an optimum Δf of 24 GHz) a modulation bandwidth of 13 GHz with a resonance frequency of 11 GHz. We speculate that the modulation bandwidth of the laser might be even larger, as we were probably limited by the bandwidth of other RF components used in our system (e.g., RF amplifier behind the photo detector, AWG roll off at high frequencies, etc.). We repeated the characterization with the lower-bandwidth AWG – modulation responses for both AWGs under optimum Δf (which was slightly lower for the lower-bandwidth AWG) are shown in Fig. 5. As we see, there is a relatively flat response up to 8 GHz for the lower-bandwidth AWG followed by a very sharp roll-off.

B. *Back-to-back performance*

To get an idea of the sensitivity of the transmitter to Δf, we plot in Fig. 6 the achieved capacity (at BER=3.8×10^{-3}) as a function of Δf. As expected from the data shown in Fig. 4, the maximum capacity (52.6 Gb/s, net capacity considering 7% FEC overhead of 48.9Gb/s) was achieved at a frequency detuning of 24 GHz. The open diamond markers show the BER of the bit-loading 52.6-Gb/s DMT signal. In practice, Δf can be controlled/tracked with a precision of better than ±1 GHz, ensuring that a capacity >50 Gb/s can easy to be achieved.

Without the OIL, a capacity of only 24.5 Gb/s (net capacity considering 7% overhead of 22.8Gb/s) was reached, mainly due to the limited modulation bandwidth shown in Fig.4. The bit loading of the 24.5 Gb/s DMT signal without OIL is shown in Fig.7 (a). The bit loading of the DMT signal with OIL and the higher-bandwidth AWG is shown in Fig. 7 (b). In these graphs, each point represents one sub-carriers and shows how many bits per symbol it carries. To achieve 1, 2, .. 6 bits per symbol, we used BPSK, QPSK, 8-QAM, 16-QAM, 32-QAM, and 64-QAM, respectively [20], [22].

The decreased performance of the higher frequency sub-carriers is mainly due to roll-off in the electrical drive signal. Up to 64-QAM modulation was achieved for good quality sub-carriers (Fig. 7 (d)). Using the low-bandwidth AWG, we obtained a capacity of 43 Gb/s (net capacity of 40Gb/s), Fig. 7 (c). The fast roll-off beyond 8 GHz is due to the limited RF bandwidth of the AWG used. Despite the lower RF bandwidth, the higher ENOB of the low-bandwidth AWG enabled 128-QAM (7 bit) modulation for subcarriers up to 2.5 GHz (Fig. 7 (c)). This clearly shows that the performance obtained with the high-bandwidth AWG was limited by its ENOB, as only 64-QAM modulation was possible. It is worth mentioning that waveform pre-distortion was not needed as the transmitter provided good modulation linearity to map the electrical DMT signal into the optical domain.

C. *Transmission Results*

The results of the transmission experiment are summarized in Table 2 and Fig. 8. After transmission thought the 500-m HC-PBGF sample, the OIL-based transmitter achieved 50.1 Gb/s (net capacity of 46.6Gb/s) using the high-bandwidth AWG, which corresponds to 95% of the BtB capacity. For transmission over the 3.8-km HC-PBGF, we obtained a capacity of 24.6 Gb/s (net capacity of 22.9Gb/s) using the low-bandwidth AWG, which corresponds to about 57% of the BtB capacity. The RF spectra of the received DMT probe signal are shown in Fig. 8 (a) and (b) for transmission over the 500-m and 3.8-km HC-PBGF samples, respectively. The corresponding bit loadings are shown in Fig. 8 (c) and (d). Comparing Fig. 8 (c) with Fig. 7 (b) we see that the capacity is lost almost independently of frequency. For the transmission through the 3.8-km HC-PBGF, we observed selective frequency fading (Fig. 8 (b)) [26] in the RF spectrum. This resulted in relatively fast changes in sub-channel capacity, Fig. 8 (d). We believe this is be due to mode coupling within the fiber (potentially due either to splicing or through point/distributed scattering) since the fiber is not strictly single-mode [7]. This remains a topic for future study. However, this observation allows us to make an important point regarding the modulation format used: DMT with bit loading is very useful in achieving high capacity transmission for channels with imperfections, as it avoids the fading frequencies and transmits more information on the best-performing subcarriers.

TABLE 2
CAPACITY ACHIEVED AFTER TRANSMISSION

	Back-to-back	After transmission
34GS/s 6-bit AWG 500-m HC-PBGF	52.6 Gb/s	50.1 Gb/s
24GS/s 8-bit AWG 3.8-km HC-PBGF	43 Gb/s	24.6 Gb/s

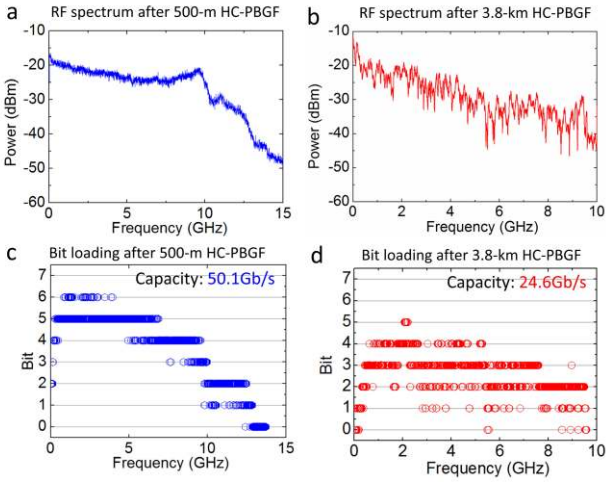

Fig. 8. (a)-(b) RF spectra of the received signal after propagation through (a) 500 m and (b) 3.8-km of HC-PBGF. (c)-(d) Bit loading of the DMT signal (each point represents one sub-carrier and shows how many bits-per-symbol it carries) for 500-m and 3.8-km transmission.

IV. CONCLUSION

An efficient high-capacity transmitter for the emerging 2 µm spectral region was demonstrated using directly modulated DMT and direct detection. To achieve this, we used optical injection locking to increase the modulation bandwidth of a state-of-the-art semiconductor laser from 4.4 GHz to 13 GHz. As a result, we obtained 52.6 Gb/s BtB capacity for single channel using a 34-GS/s 6-bit AWG. 50.1 Gb/s capacity was achieved after transmission through a 500-m long sample of HC-PBGF. Based on the same transmitter set-up, a 43 Gb/s BtB capacity was demonstrated using a 24-GS/s 8-bit AWG. 24.6 Gb/s capacity was achieved after transmission over a 3.8-km HC-PBGF, representing by far the highest length-bandwidth product at 2 µm, even when comparing this single-channel experiment with previous WDM experiments. We also showed that bit-loading directly-modulated DMT can effectively be used to mitigate selective frequency fading as observed in our longer length of HC-PBGF. Ultimately though we expect to reduce such fading through improvements in fiber fabrication and associated loss reduction.

REFERENCES

[1] R. J. Essiambre, et al., "Capacity limits of optical fiber networks," *J. Lightwave Technol.*, vol. 28, no. 4, pp. 662–701, Feb. 2010.

[2] P. Winzer, "Beyond 100G Ethernet," *IEEE Commun. Mag.* vol. 48, no. 7, pp. 26–30, Jul. 2010.

[3] A. D. Ellis, et al., "Approaching the non-linear Shannon limit," *J. Lightwave Technol.*, vol. 28, no. 4, pp. 423–433, Feb. 2010.

[4] D. J. Richardson, "Applied physics. Filling the light pipe," *Science*, vol. 330 no. 6002 pp. 327-328, Oct. 2010.

[5] T. Morioka, et al., "Enhancing optical communications with brand new fibers," *IEEE Commun. Mag.*, vol. 50, no. 2, pp. s31–s42, Feb. 2012.

[6] V. A. J. M. Sleiffer, et al., "73.7 Tb/s (96x3x256-Gb/s) mode-division-multiplexed DP-16QAM transmission with inline MM-EDFA," in *Proc. ECOC 2012*, Amsterdam, 2012, paper Th.3.C.4.

[7] F. Poletti, et al., "Hollow-core photonic bandgap fibers: technology and applications," Nanophotonics, vol. 2, no.5-6, pp. 315–340, Dec. 2013.

[8] P. J. Roberts, et al., "Ultimate low loss of hollow-core photonic crystal fibres," *Opt. Express*, vol. 13, no. 1, pp. 236-244, Jan. 2005.

[9] W. Heitmann and K.-F. Klein, "Glass for optical waveguides or the like," U.S. Patent 6490399 B1, 2002.

[10] Z. Li, et al., "Thulium-doped fiber amplifier for optical communications at 2 μm," *Opt. Express*, vol. 21, no. 8, pp. 9289–9297, Apr. 2013.

[11] Z. Li, et al., "Diode-pumped Wideband Thulium-doped Fiber Amplifiers for Optical Communications in the 1800 – 2050 nm Window," *Opt. Express*, vol. 21, no. 22, pp. 26450–26455, Nov. 2013.

[12] A. M. Heidt, et al., "High Power Diode-Seeded Fiber Amplifiers at 2 μm—From Architectures to Applications," IEEE J. Sel. Topics Quantum Electron, vol.20 , no.5, pp. 3100612-3100612, Sept./Oct., 2014.

[13] R. Phelan, et al., "$In_{0.75}Ga_{0.25}As$/InP Multiple Quantum-Well Discrete-Mode Laser Diode Emitting at 2 μm," *IEEE Photon. Tech. Lett.*, vol. 24, no. 8, pp. 652-654, Apr. 2012.

[14] N. Ye, et al., "Demonstration of 90° Optical Hybrid at 2μm Wavelength Range Based on 4×4 MMI Using Diluted Waveguide," in *Proc. ECOC 2012*, Cannes, 2014, P.2.14.

[15] A. Joshi, et al., "High-Speed, Large-Area, p-i-n InGaAs Photodiode Linear Array at 2- micron Wavelength," in *Proc. SPIE 8353, Infrared Technology and Applications*, XXXVIII, 83533D, May 2012.

[16] N. Mac Suibhne, et al., "Wavelength Division Multiplexing at 2μm," in *Proc. ECOC 2012*, Amsterdam, 2012, paper Th.3.A.

[17] N. Mac Suibhne, et al., "WDM Transmission at 2μm over Low-Loss Hollow Core Photonic Bandgap Fiber," in *Proc. OFC 2013*, Anaheim, 2013, paper OW1I.6.

[18] H. Zhang, et al., "81 Gb/s WDM Transmission at 2μm over 1.15 km of Low-Loss Hollow Core Photonic Bandgap Fiber," in *Proc. ECOC 2014*, Cannes, 2014, paper P.5.20.

[19] Z. Liu, et al., "Up to 64QAM (30 Gbit/s) Directly-modulated and Directly-detected OFDM at 2 μm Wavelength," in *Proc. ECOC 2014*, Cannes, 2014, paper Tu.4.3.5.

[20] W. Yan, et al., "80 km IM-DD Transmission for 100 Gb/s per Lane Enabled by DMT and Nonlinearity Management," in Proc. OFC 2014, San Francisco, 2014, Paper M2I.4.

[21] M. N. Petrovich, et al., "Demonstration of amplified data transmission at 2 microns in a low-loss wide bandwidth hollow core photonic bandgap fiber," Opt. Express, vol. 21 ,no. 23, pp. 28559-28569, Nov. 2013.

[22] P. Chow, et al., "A Practical Discrete Multitone Transceiver Loading Algorithm for Data Transmission over Spectrally Shaped Channels," *IEEE Trans. Commun.*, vol. 43, no. 2/3/4, pp. 773-775, Feb./March/April 1995.

[23] ITU-T Recommendation G.975.1, 2004, Appendix I.9

[24] F. Mogensen, et al., "Locking Conditions and Stability Properties for a Semiconductor Laser with External Light Injection," *IEEE J. Quantum Electron*, vol. QE-21, no. 7, pp. 784-793, Jul. 1985.

[25] E. K. Lau, et al., "Frequency Response Enhancement of Optical Injection-Locked Lasers," J. Quantum Electron., vol. 44, no.1, pp. 90-99, Jan. 2008.

[26] M. H. Hsieh, et al., "Channel estimation for OFDM systems based on comb-type pilot arrangement in frequency selective fading channels," *IEEE Trans. Consumer Electron.*, vol. 44, no. 1, pp. 217–25, Feb. 1998.

0733-8724 (c) 2015 IEEE. Personal use is permitted, but republication/redistribution requires IEEE permission. See http://www.ieee.org/publications_standards/publications/rights/index.html for more information.